

# CFD Analysis of a Stirred Vessel Bioreactor with Double Pitch Blade and Rushton Type Impellers

A. Buss<sup>1,2</sup>, A. Suleiko<sup>2,3</sup>, K. Rugele<sup>2</sup>, J. Vanags<sup>3</sup>

1. Riga Biomaterials Innovation and Development Centre, Riga Technical University, Riga, Latvia

2. Department of Chemical Engineering, Riga Technical University, Riga, Latvia

3. Latvian State Institute of Wood Chemistry, Laboratory of Bioprocess Engineering, Riga, Latvia

**Abstract:** This research presents a computer simulation investigation to develop a theoretical model to envision and understand the mixing phenomena in a stirred vessel. Mixing is required for phase homogeneity and effective heat and mass transfer within the stirred vessel. In many cases, it is challenging to obtain experimental information in a specific part of reactor and therefore the obtained results represent only average values. Also, data acquisition and interpretation can take a long time. If there is a necessity to change the geometry of a stirred vessel for scale-up purposes, then one should ensure the same reaction or process outcome is achieved as in experimental setup. Such problems can be solved at least approximately using computational fluid dynamics (CFD) model, which is less time consuming, less expensive than physical arrangement and has the capability to visualize the real system in three dimensions.

Reactor construction and impeller configurations were chosen combining best available techniques used in industry with addition of magnetic coupling for impellers. Using advanced modelling of a system the critical parameters such as impeller revolutions per minute (rpm) and operation limits can be examined. The simulation results to a certain degree are comparable with experimental results ensuring the model is fit for the purpose.

For the simulation process COMSOL Multiphysics® 5.2a with CFD module was used.

**Keywords:** CFD, eddy diffusivity, velocity profile, shear rate, torque, power, impellers, mixing, stirred vessel

## Introduction

The stirred vessel is probably the most commonly used device in the production industry. The choice of the vessel was based on availability, experience and industry standards. In this article terms vessel, tank and bioreactor have the same meaning and hence will be used interchangeably.

Bioreactors are classified in three main categories according to the operation - batch, fed-batch and continuous<sup>1</sup>. There is also a recent fourth type –

perfusion bioreactor – a successor of fed-batch reactor mainly used in biopharmaceutical industry<sup>2</sup>. The classification can be extended to the impeller type used (Rushton, pitch-blade, turbine etc.).

The mixing process in a vessel is important for effective chemical reaction, heat or mass transfer and overall homogeneity. Static parts such as baffles attached to a stirred vessel interior wall in most cases have significant effect on the mixing phenomena.

A comprehensive model of fluid dynamics can offer a significant advantage in determining the regimes of operation and hence estimating the efficiency of the operating system. For a detailed study using several parameters many measurements should be taken and the system should be observed for potential mischances of environment. The process can be enormously time consuming to collect enough data to build a model. In some situations, it is also difficult to obtain experimental information. A considerable option is to conduct pilot plant experiments but even this ordinary method has been left behind due to advancement of Computational Fluid Dynamics (CFD). A validated CFD model can support research, optimization, design scale-up and other complex engineering tasks.

In this research, COMSOL Multiphysics 5.2a has been used, where reactors with different impeller configuration and volume have been modelled to achieve a better understanding of mixing process and forces acting inside a stirred vessel.

Velocity, pressure and wall resolution profiles of the system were studied. In addition to the above profiles the following simulated plots were also added: eddy diffusivity, shear rate, power vs Reynolds number, shaft power and torque. The reactor construction was a dish bottom with three baffles and two types of double impellers (Rushton and pitched blade). The volume of stirred tank was 5 L. Mixing process was simulated at a range of revolution speeds i.e. 100-1000 rpm with 100 rpm step. Use of baffles prevent the vortex formation in the center of reactor and contribute to better mixing. The achieved results are shown in three dimensional images and Cartesian plots. The governing equations that describe mixed systems are mentioned in the following sections.

## Experimental Set-up

The experimental setup was a 5 L reactor as described above and filled with a solution resembling lysogenic broth medium for cultivation of *E. coli*<sup>3</sup>. The decoction was mixed with various speeds. The model was built as close as possible to the core experimental setup considering the key features i.e. reactor geometry and physical properties of the broth.

## Model Construction, Governing Equations and CFD Simulation

To envision the mixing process of 5 L reactor the COMSOL Multiphysics® CFD Mixer module with user modifications was used to simplify the initial model construction.

The model construction started by setting global definitions that include parameters such as vessel diameter and height, impeller and hub diameters, number of impeller blades and baffles. After setting initial definitions the reactor geometry was constructed including rotating shaft, impeller hub, impeller blades and baffles. The geometry of vessel and rotors were created using Mixer module application capabilities. The key geometry parameters are present in a table (**Table 1**).

**Table 1.** Stirred vessel geometry parameters.

Tank diameter	0.155	[m]
Tank height	0.350	[m]
Number of baffles	3	[-]
Baffle width	0.150	[m]
Impeller shaft diameter	0.020	[m]
Impeller shaft length	0.350	[m]
Impeller diameter	0.078	[m]
Impeller hub diameter	0.035	[m]
Impeller blades (Rushton)	6	[-]
Blade width	0.020	[m]
Blade length	0.020	[m]
Dish diameter	0.045	[m]
Pitch angle (pitch blade)	30	[deg]
Impeller blades (pitch blade)	3	[-]

The next step was a choice of fluid material with its corresponding properties such as density and viscosity. Those were chosen such to resemble water (i.e. 1000 kg·m<sup>-3</sup> and 0.001 Pa·s). The mixing rate was chosen at 300 rpm.

The following crucial step was to describe the physics involved in the model. This model contains a fluid domain, rotating domain, several boundary conditions including interior and exterior walls, initial values and free surface. One of the upper edge

points of the reactor was fixed as a pressure point constraint. The initial values of the velocity in every direction were set to zero.

The Navier-Stokes equations govern the motion of fluid and can be regarded as Newton's second law of motion for fluids. In the case of a compressible Newtonian fluid, this yield

$$\rho \underbrace{\left( \frac{\partial u}{\partial t} + u \cdot \nabla u \right)}_1 = \underbrace{-\nabla p}_2 + \underbrace{\nabla \cdot \left( \mu (\nabla u + (\nabla u)^T) - \frac{2}{3} \mu (\nabla \cdot u) I \right)}_3 + \underbrace{F}_4$$

where  $u$  is the fluid velocity,  $p$  is the fluid pressure,  $\rho$  is the fluid density, and  $\mu$  is the fluid dynamic viscosity. The different terms correspond to the inertial forces (1), pressure forces (2), viscous forces (3), and the external forces applied to the fluid (4). The Navier-Stokes equations were derived by Navier, Saint-Venant, Poisson and Stokes between 1827 and 1845. These equations are always solved together with the continuity equation:

$$\frac{\partial \rho}{\partial t} + \nabla \cdot (\rho u) = 0$$

The Navier-Stokes equations represent the conservation of momentum, while the continuity equation represents the conservation of mass. These equations are at the core of fluid flow modeling. Solving them, for a set of boundary conditions (such as inlets, outlets, and walls), predicts the fluid velocity and its pressure in a given geometry. Because of their complexity, these equations only admit a limited number of analytical solutions<sup>4</sup>.

The following part in construction of the model is setting the mesh (**Figure 1**) or finite element network required to solve for the defined boundary conditions. The mesh was user defined with medium-coarse size tetragonal elements to minimize the computational power (e.g. memory and simulation time) required to solve the model. The finite element method formulation of the problem results in a system of algebraic equations and yields approximate values of the unknowns at discrete number of points over the domain. That means a large problem is divided into smaller, simpler parts that are called finite elements. The simple equations that model these finite elements are then assembled into a larger system of equations that models the entire problem<sup>5</sup>.

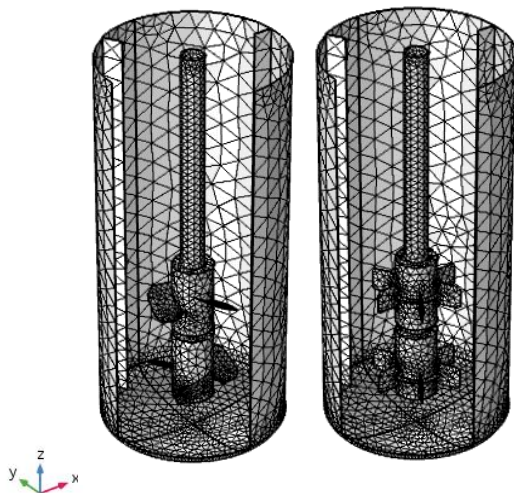


**Figure 1.** Stirred vessel (5 L) meshed geometries with pitch blade (left) and Rushton impellers (right).

The final part of the model setup was a choice of the study. This research is using a frozen rotor study available in COMSOL Multiphysics®. The frozen rotor study is used to compute the velocity, pressure, turbulence, concentration, temperature, and other fields for flow in rotating machinery and is a special case of a stationary study. The rotating parts are kept frozen in position, and the rotation is accounted for by the inclusion of centrifugal and Coriolis forces. The study is especially suited for flow in rotating machinery where the topology of the geometry does not change with rotation. It is also used to compute the initial conditions for time-dependent simulations of flow in rotating machinery.

When all these steps are done correctly then the computation may begin. Depending on computational power this step can take up to several hours. During this process, large amount of computer RAM (more than 10 GB) can significantly reduce computational time. Considering the huge computational power on demand it is worth to consider running the simulation on Amazon Elastic Compute Cloud™ (Amazon EC2)™ or Linux cluster.

### Simulation Results and Discussion

After completion of simulation several graphical representations and plots were acquired. The representative graphics were obtained using 300 rpm impeller speed and double pitch blade and Rushton type impellers. The plots were created using parameter sweep for the 100-1000 rpm range.

**Velocity field:** this graphical representation demonstrates how vorticity affects the mixing phenomena. The cut plane was made along XZ-plane

to demonstrate the cross-section of the reactor. The front walls were made invisible to observe the inside of reactor model. The combined streamline plot demonstrates fluid movement during mixing. Streamlines has random directions indicating that the fluid is well mixed in both cases. Baffles significantly minimize fluid compartmentation and the formation of vortex along the reactor shaft. The fluid velocity is higher near the blades.

Surface: Velocity magnitude (m/s) Streamline: Velocity field (Spatial)

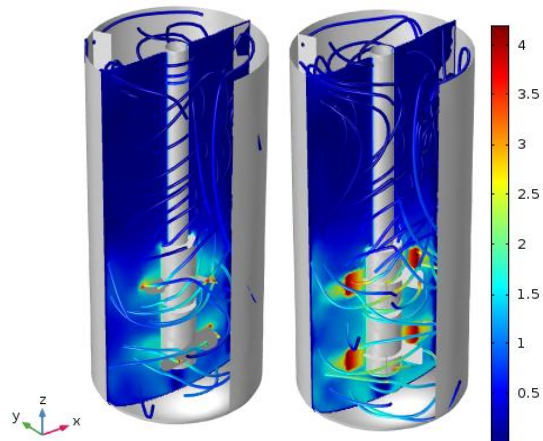


**Figure 2.** Velocity and streamline profiles for pitch blade and Rushton impeller designs at 300 RPM.

**Slice plot:** shows a cross-sectional surface that indicates how a variable change over a distance (XZ-plane along Y-axis). Three parallel vertical slices are implemented through the whole diameter of the reactor. The fluid velocity is higher near the impeller and gradually reduces near the reactor wall.

Slice: Velocity magnitude (m/s)

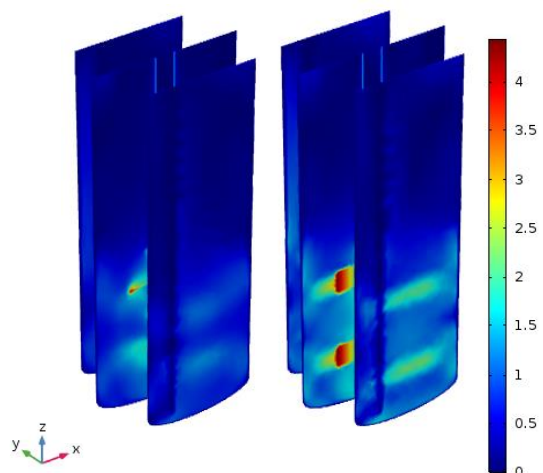


**Figure 3.** Slice plot in XZ-plane (distributed along Y-axis).

**Pressure contour:** This graphical representation demonstrates the distribution of pressure inside the stirred vessel. From the color legend, it can be



noticed that the higher pressure is exerted on certain parts of blades as they rotate and on the bottom part of reactor near the walls caused by the fluid column.

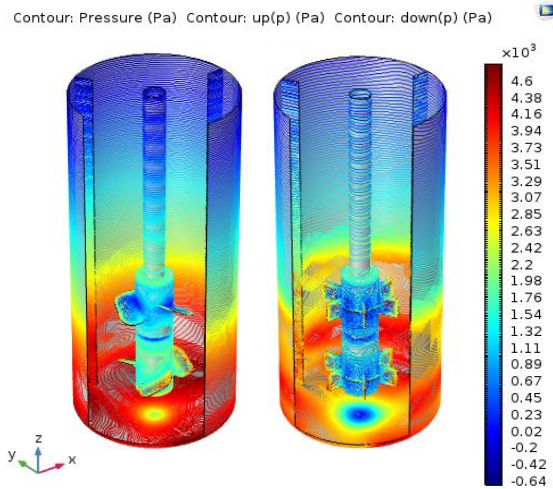


Figure 4. Pressure distribution contours.

Interestingly there is pressure drop in the center directly under the reactor shaft. That can be explained by formation of slight cavitation as the radial Rushton impeller is pushing the fluid away from the center towards the walls. In the case of pitch blade design this effect is less noticeable but still present as the pitch blade impeller is an axial impeller.

**Wall resolution:** or a non-dimensional wall distance for a wall-bounded flow can be defined in the following way:

$$y^+ \equiv \frac{u_* y}{\nu}$$

where  $u_*$  is the friction velocity at the nearest wall,  $y$  is the distance to the nearest wall and  $\nu$  is the local kinematic viscosity of the fluid.  $y^+$  is commonly used in boundary layer theory and in defining the law of the wall<sup>6</sup>. It is often used to describe how coarse or fine a mesh is for a flow pattern. Wall resolution shows the shear stress at a wall node.

Wall resolution is necessary to verify that the solution is reasonably accurate for the current mesh. The dimensionless distance number (Figure 5) shows how far into the boundary layer the computational domain starts and should not be too large (less than 100). In our case the range does not exceed 40 and hence the mesh size for both models can be considered adequate. Therefore, there is no necessity to create a finer mesh that would significantly increase the computation time with little accuracy benefits. One should consider refining mesh size in the wall normal direction if there are regions where the wall resolution exceeds several hundred. Notice that wall resolution is higher in the case of Rushton

turbine due to its stronger influence on the orthogonal walls.

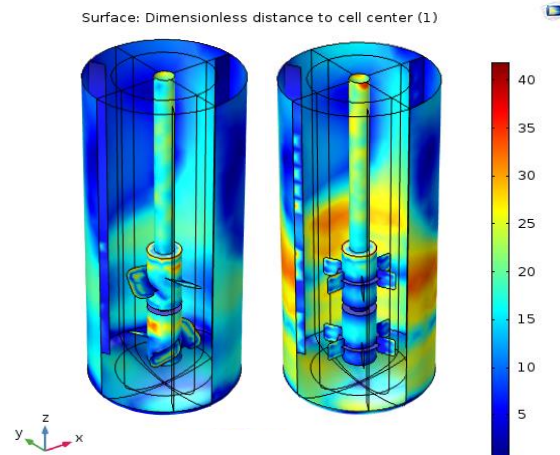


Figure 5. Dimensionless distance to the cell (reactor) center.

**Eddy diffusivity:** demonstrates a diffusion process by which substances are mixed in the fluid system due to eddy motion (Figure 6). The white arrows indicate the direction of fluid motion which flows from the impeller blades towards the walls and then distributes upwards and downwards transforming into spirals - a typical pattern for radial impellers. The highest eddy motion is near the blades and between both impellers.

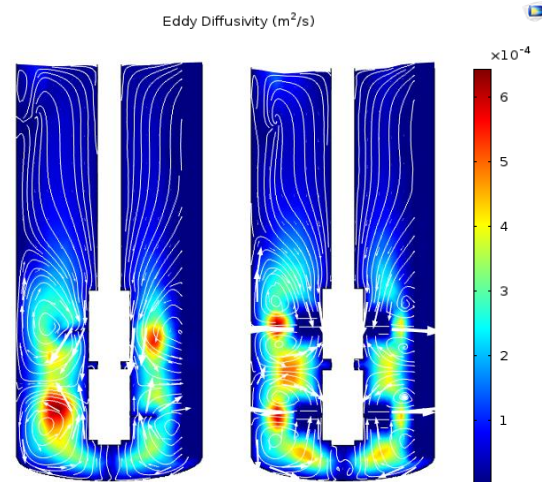


Figure 6. Eddy motion along XZ-plane at 300 RPM.

**Shear rate:** is a rate of change of velocity at which one layer of fluid passes over an adjacent layer (Figure 7). This plot was also evaluated along the XZ-plane using a logarithmic scale as the values near the blades and walls differ considerably. The plots show a significant shear rate on the impeller blades as there is the highest friction between the fluid layers.

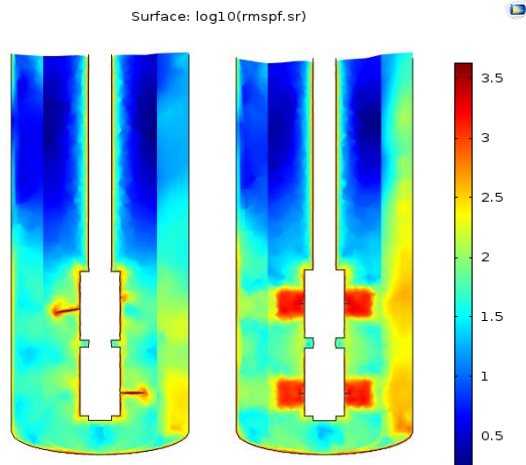


Figure 7. Shear rate along XZ-plane at 300 RPM.

Besides the surface and space graphs several simulated Cartesian plots were also obtained.

**Shaft rotation power:** shows a shaft power versus a range of rpm. The power raises exponentially as the frequency of rotation (rpm) increases (Figure 8). Comparing with experimental results the maximum power drawn was about two times lower. Discrepancies may arise from modeled and actual differences in density and viscosity of fluid. There is considerably more power drawn when using a Rushton turbine.

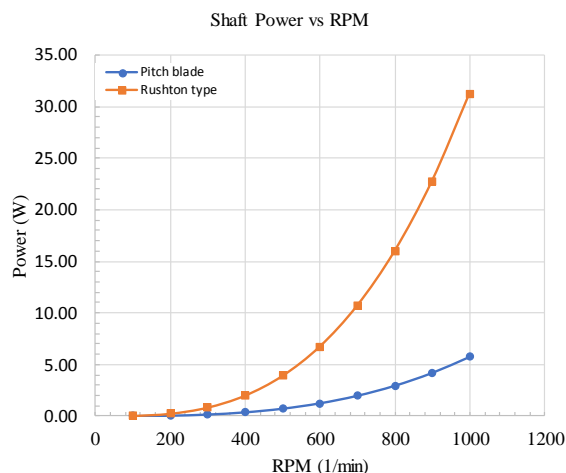


Figure 8. Modelled shaft power evaluation versus frequency of rotation (rpm).

**Impeller torque:** represents an impeller torque versus a range of rpm. Similarly, to the power plot the torque rises exponentially as the rpm increases (Figure 9). The maximum torque is less than two times lower comparing to experimental results. The reasons might be the same as in the case with shaft power.

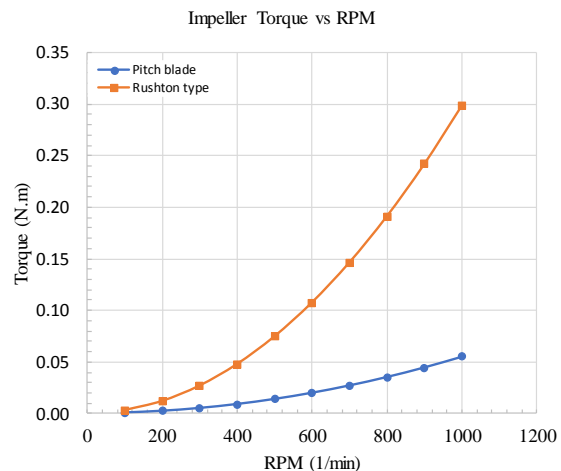


Figure 9. Modelled impeller torque evaluation vs rpm.

**Power number vs Reynolds Number:** shows the relationship between two dimensionless numbers – Power number  $Np$  and Reynolds number  $Re$ . The plot follows the typical pattern of the Rushton turbine (Figure 10) and the pitch blade turbine (Figure 11). For the Rushton turbine as the  $Re$  increases the  $Np$  decreases rapidly in the laminar region ( $Re < 20\,000$ ) then the decrease slows into laminar-turbulent transition region ( $20\,000 < Re < 40\,000$ ) and become relatively constant in the turbulent region ( $Re > 50\,000$ ). For the pitch blade turbine  $Np$  decreases logarithmically as  $Re$  increases. This behavior and the  $Np$  values agrees with previous studies in this field<sup>7</sup>.

$Np$  is calculated by the following expression:

$$Np = \frac{P}{\rho \cdot n^3 \cdot D^5}$$

where  $P$  is power,  $\rho$  is fluid density,  $n$  – rotational speed ( $s^{-1}$ ) and  $D$  is impeller diameter.  $Np$  has no units.

$Re$  is defined as:

$$Re = \frac{\rho \cdot n \cdot D^2}{\mu}$$

where  $\mu$  is dynamic viscosity.  $Re$  same as  $Np$  is dimensionless.

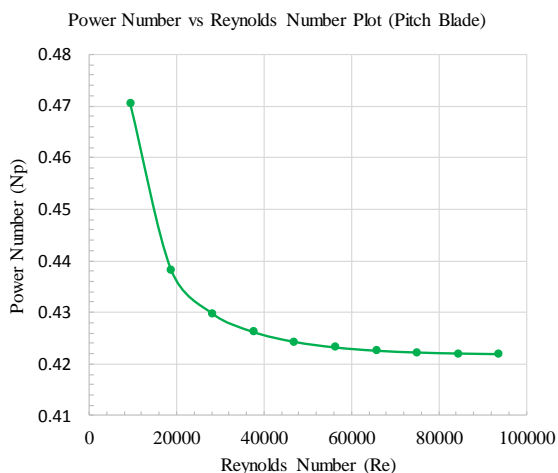


**Figure 10.** Simulated power number versus Reynolds number plot for the pitch blade turbine.

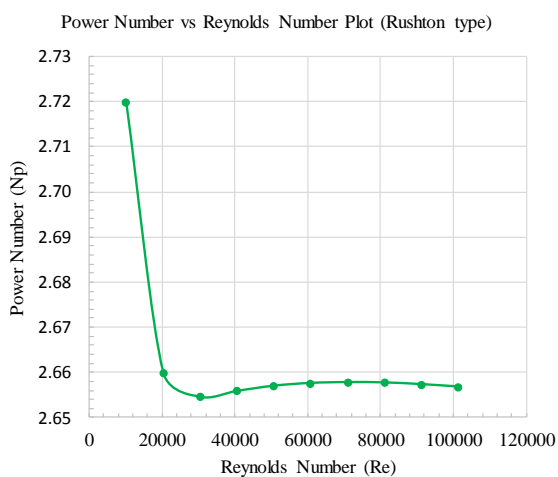


**Figure 11.** Simulated power number versus Reynolds number plot for Rushton blade turbine.

## Conclusions

Several 3D plots and 2D cross section profiles of a 5 L stirred vessel has been investigated using COMSOL Multiphysics® and computational fluid dynamics (CFD). The purpose of these experiments was to envision what effects the different type impellers have on the mixed fluid and thus enable to understand the mixing phenomena better.

The results are shown in the form of velocity and streamline plots, slice diagrams and graphs. Eddy motion, slice and shear rate profiles indicate that Rushton turbine constitutes to better mixing as the fluid motion vectors reach the reactor walls and the most remote bottom corners with greater force comparing to the pitch blade impeller; however, higher shear stress especially near the blades may be damaging to shear sensitive cell cultures. Cartesian

plots also demonstrate that Rushton turbine draws significantly more power as the RPM increases.

The pitch blade turbine has less overall shear rate and more uniform energy distribution deeming it better suited for shear sensible cultures.

The overall simulation results are in reasonable agreement with theory, however the shaft power and torque results appear somewhat lower than the measured values.

Future work can be aimed towards the scale-up of the bioreactor and investigation of the 2D and 3D profiles above using COMSOL® time dependent study. In the actual reactor, the impellers are held in place by magnetic force. High rotational speeds or viscosity can overcome this force and cause the impeller to skid around the shaft which is undesirable. Modelling the forces that induce skidding of magnetically coupled impellers is another prospect.

## References

1. Nienow, A. W. Stirring and stirred-tank reactors. *Chemie-Ingenieur-Technik* **86**, 2063–2074 (2014).
2. Bonham-Carter, J. & Shevitz, J. How High-Concentration Cultures Will Characterize the Factory of the Future. *24 BioProcess Int.* **9**, (2011).
3. Bertani, G. Lysogeny at mid-twentieth century: P1, P2, and other experimental systems. *J Bacteriol* **186**, 595–600 (2004).
4. COMSOL. What Are Navier-Stokes Equations. (2017). Available at: <https://www.comsol.com/multiphysics/navier-stokes-equations>. (Accessed: 1st August 2017)
5. Logan, D. *A first course in the finite element method*, 4–23, Cengage Learning, Stamford, (2012).
6. CFD Online. Dimensionless Wall Distance (y plus). (2017). Available at: [https://www.cfd-online.com/Wiki/Dimensionless\\_wall\\_distance\\_\(y\\_plus\)](https://www.cfd-online.com/Wiki/Dimensionless_wall_distance_(y_plus)). (Accessed: 31st July 2017)
7. Nienow, A. W. & Miles, D. Impeller Power Numbers in Closed Vessels. *Ind. Eng. Chem. Process Des. Dev.* **10**, 41–43 (1971).

## Acknowledgements

This work has been supported by European Regional Development Fund within the project “Influence of the magnetic field initiated stirring on biotechnological processes” No. 1.1.1.1/16/A/144.